ELSEVIER

Journal of Organometallic Chemistry 635 (2001) 100–109

Journal of Organometallic Chemistry

www.elsevier.com/locate/jorganchem

Methane inversion on transition metal ions: a possible mechanism for stereochemical scrambling in metal-catalyzed alkane hydroxylations

Kazunari Yoshizawa

Institute for Fundamental Research of Organic Chemistry, Kyushu University, Fukuoka 812-8581, Japan

Received 3 April 2001; accepted 9 May 2001

Dedicated to Professor M.J.S. Dewar on the occasion of the 50th anniversary of his landmark paper

Abstract

The configurational inversion of both free methane and methane bound to first-row transition-metal ions is discussed using the density functional theory (DFT) calculations at the B3LYP level of theory. Computed transition states for the inversion of methane on the $M^+(CH_4)$ complexes have C_s structures in which one pair of C–H bonds is about 1.2 Å in length and the other pair is about 1.1 Å, where M is Sc, Ti, V, Cr, Mn, Fe, Co, Ni, and Cu. The barrier height for the methane inversion decreases significantly from 109.4 kcal mol^{-1} for free methane to 17–23 kcal mol^{-1} for the late transition-metal complexes, $Fe^+(CH_4)$, $Co^+(CH_4)$, $Ni^+(CH_4)$, and $Cu^+(CH_4)$. The computational results suggest that the inversion can occur under ambient conditions through a thermally accessible transition state, and it may lead to an inversion of stereochemistry at a carbon atom of substrate if an alkane-complex is formed as a reaction intermediate in C–H bond activation reactions. We propose that a radical mechanism based on a planar carbon species may not be the sole source of the observed loss of stereochemistry in transition-metal catalyzed alkane hydroxylation reactions and other related reactions.

Keywords: Alkane hydroxylation; Molecular orbital theory; Methane activation; Stereochemical scrambling

1. Introduction

The synthesis of compounds containing a planar-tetracoordinate carbon, the so-called 'anti van't Hoff/LeBel structure', that are stable enough to be isolated and characterized under ambient conditions has continued to be a challenging target [1]. In 1970, Hoffmann et al. suggested the transformation of tetrahedral to planar methane through a symmetry-allowed process for either a twisting ($T_d \rightarrow D_2 \rightarrow D_{4h}$) or a squashing ($T_d \rightarrow D_{2d} \rightarrow D_{4h}$) pathway [2]. The fragment molecular orbital (FMO) diagram in Chart 1 leads to the molecular orbitals (MOs) of a tetrahedral AH_4 molecule. This simple diagram shows that the a_1 and t_2 orbitals of the H_4 fragment combine in-phase (out-of-phase) with the s, p_x, p_y, and p_z atomic orbitals of A to form the MOs $1a_1$ and $1t_2$ ($2a_1$ and $2t_2$), respectively [3]. Eight-electron AH_4 molecules such as methane, silane, and germane are very stable in their tetrahedral structures, owing to the low-lying threefold degenerate $1t_2$ HOMO that has an A–H bonding character. The sequence of the unoccupied MOs $2a_1$ and $2t_2$ can be changed, depending on the molecule and methodology used, but this is not an important point in discussing the stability of these molecules.

Chart 2 shows how the MOs of the square-planar H_4 fragment correlate with the s, p_x, p_y, and p_z atomic orbitals of A to form the MOs of a D_{4h} square-planar AH_4 molecule. The three bonding $1a_{1g}$ and $1e_u$ orbitals are low-lying in energy, and the subsequent a_{2u} and b_{1g} orbitals are essentially nonbonding in the D_{4h} structure [4]. Extended Hückel calculations predicted that T_d methane is more stable than the D_{4h} square-planar methane by 127 kcal mol^{-1} [3]. CNDO and approximate ab initio Hartree–Fock (HF) calculations yielded 187 and 249 kcal mol^{-1}, respectively, for the same

E-mail address: kazunari@ms.ifoc.kyushu-u.ac.jp (K. Yoshizawa).

0022-328X/01/$ - see front matter
PII: S0022-328X(01)00995-0

quantity [3,5]. Extensive ab initio calculations by Schleyer and collaborators [6] gave 240 kcal mol^{-1} at the HF/STO-3G level, 168 kcal mol^{-1} at the HF/4-31G level, 171 kcal mol^{-1} at the HF/6-31G* level, and 160 kcal mol^{-1} at the MP2/6-3lG* level of theory.

However, Gordon and Schmidt [7] demonstrated from detailed analyses of Hessians (matrix of energy second derivatives) [8] that the D_{4h} planar structure is not a true transition state for the inversion of methane.

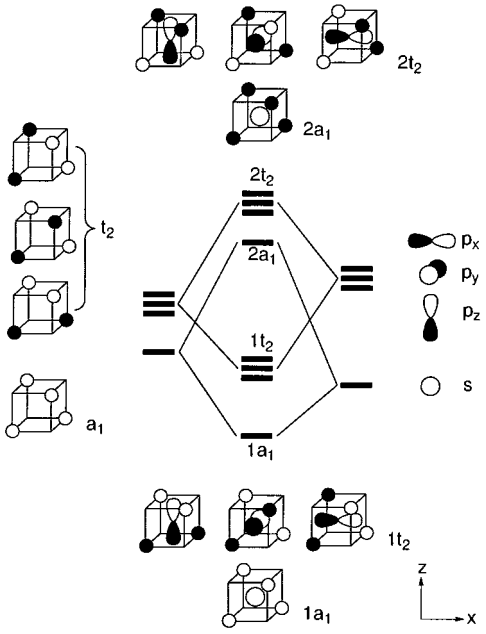

Chart 1.

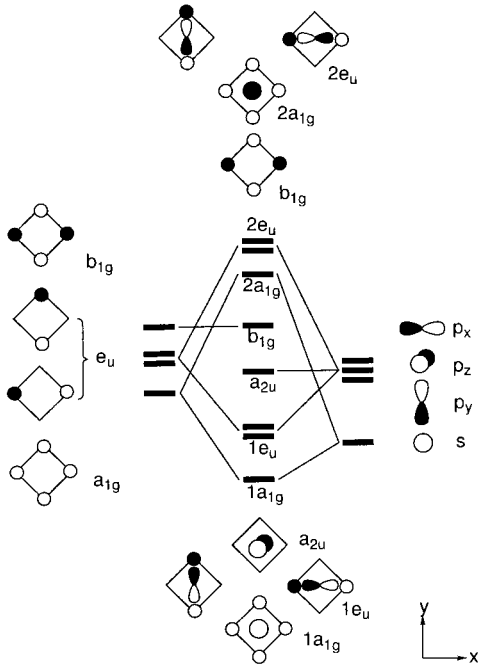

Chart 2.

This was an important discovery in computational quantum chemistry. The ^1A_g state with a D_{4h} structure has four imaginary vibrational modes of B_{2u}, A_{2u}, and degenerate E_u symmetry. As a true transition state, a saddle point on a potential energy surface should have only one imaginary mode of vibration, the D_{4h} planar structure is not a transition state for the inversion of methane. The true inversion transition state was found to have a distorted C_s structure, which is quite different both geometrically and energetically from the D_{4h} transition state presumed earlier. This C_s transition state is 117.0–125.6 kcal mol^{-1} higher in energy than the global minimum of the T_d structure at the MCSCF/TZV + + G(d,p), SOCI/TZV + + G(d,p), and SOCI/TZV + + G(d,p) with Davidson correction levels of theory. Detailed theoretical analyses on the inversion of methane were also reported by Schleyer et al. [9]. As the barrier height is larger than the C–H bond dissociation energy of 104 kcal mol^{-1}, methane is unlikely to undergo such interesting inversion under ambient conditions.

There has been a great interest in the C–H activation of small alkanes particularly methane, with the development of selective conversion of natural gas to liquid fuels in mind. Cytochrome P450 [10] and soluble methane monooxygenase (MMO) [11], which involve iron-oxo species as active catalytic centers, are excellent biological catalysts for selective alkane oxidation, although P450 is unable to activate methane. Accumulated studies have shown that P450- and MMO-catalyzed hydroxylation reactions proceed with loss of stereochemistry at a carbon atom of the substrate. Stereochemical scrambling was first observed by Groves et al. [12] in the hydroxylation of *exo*-tetradeuterated norbornane by rabbit liver microsomes P450. Moreover, the hydroxylation of ethylbenzene by P450 was reported to proceed with 23–40% loss of stereochemistry [13]. In addition, in hydroxylation reactions by soluble MMO, ca. 20–40% inversion of stereochemistry has been observed at the labeled carbon atoms [14]. The relatively high degree of inversion observed could be ascribed to flipping of a substrate intermediate that has a sufficiently long lifetime to undergo configurational inversion. Therefore, it is generally believed that the loss of stereochemistry requires a nonconcerted mechanism via a carbon radical as an intermediate species because a carbon atom bearing an unpaired electron is planar. This radical mechanism is called the 'oxygen rebound mechanism' [10].

Siegbahn et al. [15], Yoshizawa and coworkers [16], Morokuma et al. [17], and Friesner et al. [18] have investigated, from quantum chemical calculations, the mechanism of methane hydroxylation mediated by soluble MMO. The issue of whether a methane molecule prefers to form a complex with the metal active site or it prefers to interact directly with the oxo ligand is a

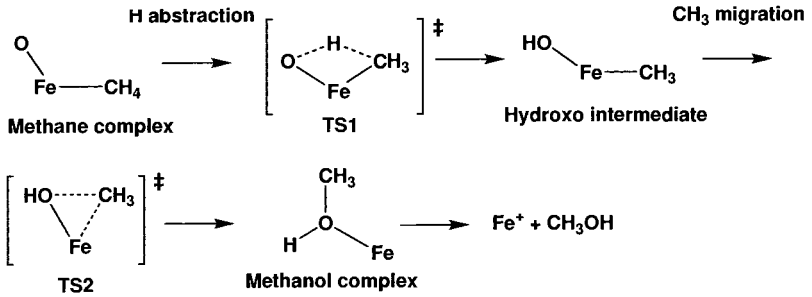

Scheme 1.

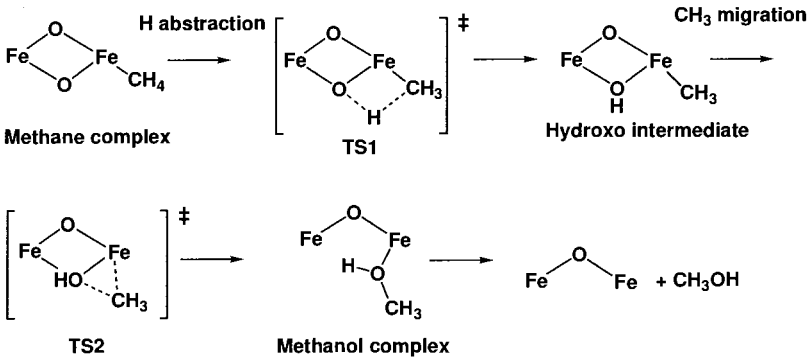

Scheme 2.

crucial point in the hydroxylation mechanism. We think that the key to understanding the methane hydroxylation mechanism is a simple gas-phase reaction. Schröder and Schwarz [19] demonstrated that the bare FeO^+ complex, generated under ion cyclotron resonance conditions, successfully converts methane to methanol in high yield. From the detailed density functional theory (DFT) calculations we have proposed a 'two-step concerted' mechanism for the methane–methanol conversion by the iron-oxo species [20]; in this mechanism, neither the radical nor the ionic intermediate is formed, as indicated in Scheme 1. An important point of our proposal is that methane is activated on a coordinatively unsaturated iron-oxo species to form a methane complex and that the two-step concerted processes lead to the methane–methanol conversion at the transition-metal active center.

We have applied the mechanism indicated above to methane hydroxylation by soluble MMO. As shown in Scheme 2, we demonstrated from the DFT [16] and extended Hückel [21] computations that the methane–methanol conversion can occur through the formation of a methane complex on the diiron active site of intermediate **Q** of soluble MMO, which has been proposed to have a $Fe_2(\mu\text{-}O_2)$ diamond core [22], in a way similar to the gas-phase reaction indicated in Scheme 1. Ancillary ligands are not present in Scheme 2; but in our actual DFT computations four- and five-coordinate irons were assumed for the diiron model complex, according to the report by Que et al. [22]. Our discussion may be restricted to nonheme enzymes, the metal active sites of which are relatively flexible and coordinatively unsaturated in some cases, and may not be extended to heme enzymes that involve a rigid six-coordinate iron site. From DFT computations Shaik and coworkers have suggested that interactions of the substrate with the oxo ligand play a crucial role in alkane hydroxylation by cytochrome P450 [23].

We are interested in the inversion of methane to rationalize the 'two-step concerted' mechanism in MMO-mediated hydroxylation reactions that proceed with 20–40% inversion of stereochemistry [14]. As the C–H bonds of methane are weakened on transition-metal complexes, we consider that the barrier height of the methane inversion should be significantly decreased. The purpose of our work is to investigate whether or not the inversion of methane can occur at transition-metal active centers under ambient conditions through a thermally accessible, low-lying transition state. If the mechanism postulated by us is viable, then a radical mechanism based on a planar carbon species may not be the sole source of the observed loss of stereochemistry in transition-metal catalyzed alkane hydroxylation reactions and other related reactions. We discuss the potential meaning of this interesting reaction. This paper is a short review of our recent work [16,20,24].

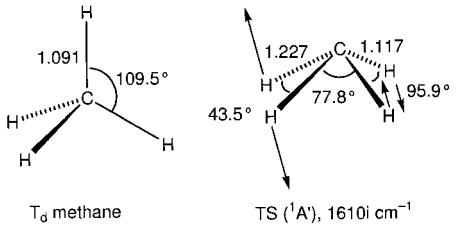

Fig. 1. Geometries of the T_d global minimum and the C_s transition state for the inversion of free methane. The bond lengths are in Å, and the bond angles (italic) are in degrees. The arrows in the transition state indicate the transition vector.

2. Method of calculation

We used the hybrid (DFT/HF) method of Becke [25] and Lee, Yang, and Parr (LYP) [26], the so-called B3LYP method, which consists of the Slater exchange, the HF exchange, the exchange functional of Becke, the correlation functional of LYP, and the correlation functional of Vosko et al. [27]. In general, this hybrid method has provided, excellent descriptions of many reaction profiles, particularly in molecular geometries, heats of reaction, and activation energies of transition states [28]. For the first-row transition metals we used the (14s9p5d) primitive set of Wachters [29] supplemented with one polarization f-function ($\alpha = 0.60$ for Sc, 0.69 for Ti, 0.78 for V, 0.87 for Cr, 0.96 for Mn, 1.05 for Fe, 1.17 for Co, 1.29 for Ni, and 1.44 for Cu) [30] resulting in a (611111111 | 51111 | 311 | 1) [9s5p3d1f] contraction, and for the H and C atoms we used the 6-311G** basis set of Pople and coworkers [31]. Vibrational frequencies were computed to ensure that on a potential energy surface all optimized geometries correspond to a local minimum that has no imaginary frequency or a saddle point that has only one imaginary frequency. Zero-point vibrational energy corrections were taken into account in calculating the total energies of the reactant (= product) complexes and the transition states. The spin-unrestricted method was applied to the open-shell systems. These DFT computations were performed using the GAUSSIAN 94 program package [32]. To draw a better picture for the interesting transition state, we carried out the orbital interaction analyses based on the extended Hückel method [33], implemented with YAeHMOP [34].

3. Results and discussion

3.1. Inversion of free methane

First let us look at the inversion of methane, which was calculated and analyzed with high-level ab initio methods [7,9]. We successfully reproduced the true transition state as well as the reaction pathway for the inversion of free methane with the B3LYP DFT method and the 6-311G** basis set [24a]. It was shown that the closed-shell ^1A_g state with a planar D_{4h} structure has three imaginary vibrational modes and that the A″ state with a C_s structure has only one imaginary mode, the C_s transition state lying 21.4 kcal mol^{-1} below the D_{4h} methane. Fig. 1 shows optimized geometries for the T_d global minimum and the C_s transition state of methane, in which the imaginary mode of vibration is indicated for the transition state. As this C_s structure has only one imaginary mode of 1610i cm^{-1}, it is the true transition state for the configurational inversion of methane. One pair of C–H bonds of the C_s transition state is 1.227 Å in length and the other pair is 1.117 Å. The bond angle of H–C–H for the long C–H pair is 43.5° and that for the short C–H pair is 95.9°. This structure can be regarded as a complex between the singlet methylene and H_2 [9]. The activation barrier for this transition state was computed to be 109.4 kcal mol^{-1} with zero-point vibrational energy corrections. This barrier height is a little larger than the energy required to break a C–H bond of methane (104 kcal mol^{-1}). Thus, these B3LYP DFT computational results are in good agreement with the earlier high-level, multiconfigurational analyses by Gordon and Schmidt [7] and Schleyer et al. [9].

It was confirmed from an intrinsic reaction coordinate [35] analysis that this transition state connects the equivalent T_d global minimum correctly in both the forward and reverse directions [24a]. Scheme 3 shows the complicated geometrical change that leads to the inversion of methane via the C_s transition state. Thus, we are able to derive reasonably excellent descriptions of the inversion of methane from B3LYP DFT computations, particularly in the molecular geometries, the reaction pathway, and the activation energy of the transition state. The method chosen is therefore appropriate for the topic addressed in this paper.

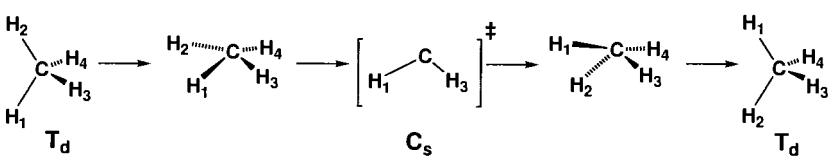

Scheme 3.

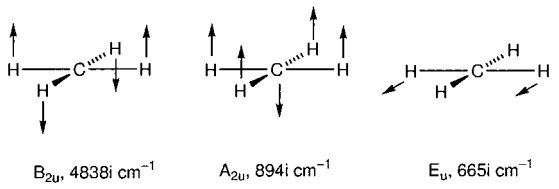

Fig. 2. Imaginary B_{2u}, A_{2u}, and degenerate E_u vibrational modes of D_{4h} methane at the B3LYP/6-311G** level of theory.

As established in previous studies [7,9], the D_{4h} structure of methane has four imaginary vibrational modes of B_{2u}, A_{2u}, and degenerate E_u symmetry, which suggests that there are stationary structures of lower energy in addition to the global minimum T_d structure. The imaginary modes and the wave numbers from our B3LYP calculations are shown in Fig. 2. The methane B_{2u} mode of 4838i cm^{-1} corresponds to the $D_{4h} \rightarrow T_d$ transformation; the A_{2u} mode of 894i cm^{-1} corresponds to the $D_{4h} \rightarrow C_{4v}$ transformation; and the degenerate E_u mode of 665i cm^{-1} corresponds to the $D_{4h} \rightarrow C_{2v}$ transformation. It is therefore interesting to look at the Walsh diagrams as well as the total energy changes with respect to the $T_d \rightarrow D_{4h}$, $D_{4h} \rightarrow C_{4v}$, and $D_{4h} \rightarrow C_{2v}$ geometrical changes of methane.

Fig. 3 presents the Walsh diagrams computed at the HF level with the 6-311G** basis set. The solid lines indicate one-electron energies in units of electron volts, and the dotted lines indicate the relative total energies in units of kilocalories per mole. The energies of the one-electron orbitals and the total energies measured from the T_d ground state are indicated on the left and right, respectively. The first Walsh diagram shows that methane strongly resists the D_{4h} deformation. In the course of this transformation, two members of the $1t_2$ HOMO are slightly stabilized in energy leading to the $1e_u$ orbital; but the third member is destabilized significantly leading to the nonbonding a_{2u} orbital, which is the principal reason that the D_{4h} form is energetically unstable compared with the T_d form because all bonding between the p orbital of the carbon atom and the s orbitals of the hydrogen atoms is lost by this geometrical change [2]. During the same deformation, one member of the $2t_2$ orbital set is stabilized to form the b_{1g} orbital in the D_{4h} structure. This is the other nonbonding orbital in planar methane. Consequently, the HOMO(a_{2u})–LUMO(b_{1g}) gap for the D_{4h} structure of methane is decreases significantly.

Having described the Walsh diagrams along the $T_d \rightarrow D_{4h}$ reaction coordinate, we next follow one-electron orbitals along the other two reaction coordinates. Let us look at the $D_{4h} \rightarrow C_{4v}$ change. The total energy of methane decreases on the $D_{4h} \rightarrow C_{4v}$ pyramidalization by about 20 kcal mol^{-1}, as indicated by the dotted lines in Fig. 3. Thus, methane prefers this C_{4v} deformation. The MOs of square-pyramidal methane are shown

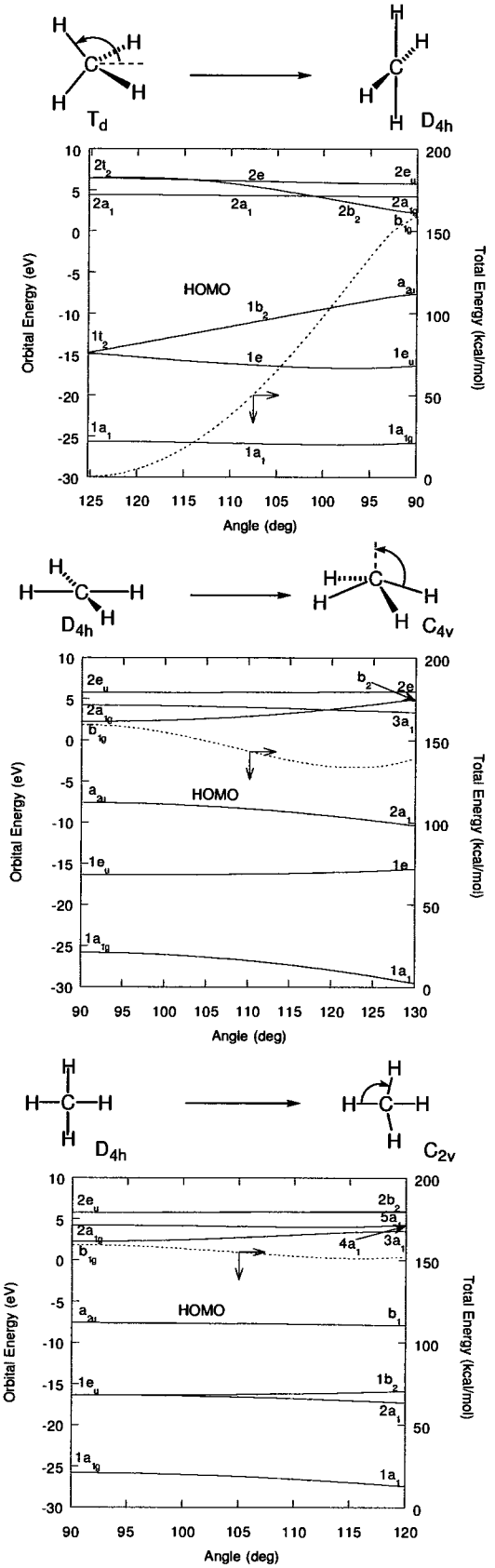

Fig. 3. Walsh diagrams for the $T_d \rightarrow D_{4h}$, $D_{4h} \rightarrow C_{4v}$, and $D_{4h} \rightarrow C_{2v}$ transformations of methane at the HF level of theory.

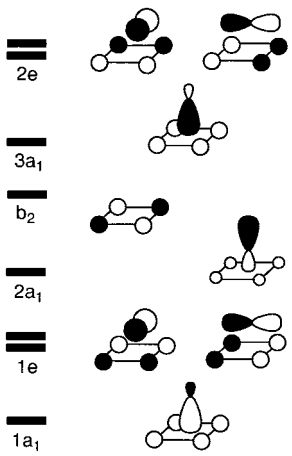

Chart 3.

in Chart 3. The a_{2u} HOMO of D_{4h} methane is stabilized in energy through relaxation to the pyramidal structure and the resulting $2a_1$ HOMO of C_{4v} methane acquires considerable s hybridization and H–H in-phase interactions [6b]. This electronic process is therefore symmetry allowed for methane and the total energy of methane decreases along this reaction coordinate. In remarkable contrast to methane, the total energies of silane and germane increase considerably on the $D_{4h} \rightarrow C_{4v}$ pyramidalization [24b]. There is a crossing between the HOMO and the LUMO in each case, and therefore the $D_{4h} \rightarrow C_{4v}$ pyramidalization is a symmetry-forbidden electronic process for silane and germane. Therefore, this geometrical transformation requires high activation energy in silane and germane.

The Walsh diagram along the $D_{4h} \rightarrow C_{2v}$ reaction coordinate of methane shows that the a_{2u} level of D_{4h} methane remains almost unchanged in energy, but one member of the $1e_u$ set and the $1a_{1g}$ orbital decreases slightly along this reaction coordinate, and the total energy decreases slightly accordingly, as indicated by the dotted line. Thus, methane also prefers the C_{2v} deformation. Here we can derive, from these Walsh diagram analyses, an important conclusion with respect to the transition-state structure for the configurational inversion of methane. As the C_{4v} and the C_{2v} deformations are symmetry allowed for methane, in remarkable contrast to silane and germane, the interesting C_s transition state for the methane inversion is a consequence of a significant mixture of both C_{4v} and C_{2v} structures with the square-planar D_{4h} structure [24b].

3.2. Methane inversion on the $M^+(CH_4)$ complexes

Having described the inversion of free methane, let us next consider how differently the inversion of methane proceeds at transition-metal active centers [24a]. Alkane-complexes are accepted intermediates proposed to be involved in C–H bond activation reactions. The binding of methane to Sc^+, Fe^+, Co^+, Rh^+, and Ir^+ has been theoretically studied by Morokuma and coworkers [36]. Recently, related methane-complexes have been extensively investigated using modern spectroscopic techniques [37]. Billups et al. reported low-temperature photolysis of CH_3CoH to give the $Co(CH_4)$ complex [37i]; their FTIR matrix isolation spectroscopy in solid argon demonstrated that methane is distorted significantly on this σ-complex. It is therefore of general interest to consider whether or not the inversion of methane occurs at the transition-metal active center of the complex. Our main purpose of this short review is to look at whether or not the barrier height for the methane inversion is decreased from the value for free methane (109.4 kcal mol^{-1}) so that it could serve as a thermally accessible, low-lying transition state.

Before we present the DFT computational results, it is useful to consider the activation of methane from a point of view of its MOs. The MOs of methane are indicated in Chart 1. It is essential for our discussion to note that the occupied orbitals are C–H bonding (in-phase) and that the unoccupied orbitals are C–H antibonding (out-of-phase). The HOMO–LUMO gap is about 20 eV at the extended Hückel level of theory, and therefore methane is a very hard hydrocarbon with strong C–H bonds. In view of these frontier orbitals, the C–H bonds of methane can be weakened when the LUMO or the HOMO is partly filled and partly unfilled, respectively, because of electron transfer or orbital interaction with other molecules, particularly with transition-metal complexes. The C–H bonds of methane are activated on transition-metal complexes because of both the electron transfer from the methane t_2 HOMO to the unfilled d-block orbitals of the complex and the electron transfer from the filled d-block orbitals to the unoccupied orbitals of methane. On the basis of such an orbital interaction picture, we have discussed the activation of methane and its conversion to methanol on the diiron active site of soluble methane monooxygenase (MMO) [21]. We can expect that the formation of methane σ-complex should result in small activation energy for the inversion of methane because the C–H bonds of methane are weakened owing to orbital interactions.

We carried out systematic B3LYP computations on the $M^+(CH_4)$ σ-complexes and the transition states for the inversion of methane on the complexes, in which M^+ is the first-row transition-metal ions from Sc^+ to Cu^+ [24a]. Computed values of the activation energies (ΔE_1 and ΔE_2) for the inversion of methane on the $M^+(CH_4)$ complexes are listed in Table 1, where ΔE_1 is the value measured from the methane complex and ΔE_2 is the value relative to the dissociation limit. As expected, the activation energy (ΔE_1) decreases significantly from 109.4 kcal mol^{-1} for free methane to less

Table 1
Computed barrier heights (in kcal mol^{-1}) for the inversion of methane on the $M^+(CH_4)$ complexes, in which M^+ is the first-row transition-metal ions

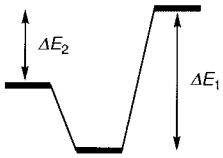

Complex	Low spin	High spin
ΔE_1		
$Sc^+(CH_4)$	64.1 (^{1}A′)	64.8 (^{3}A″)
$Ti^+(CH_4)$	58.8 (^{2}A″)	55.4 (^{4}A′)
$V^+(CH_4)$	64.6 (^{3}A′)	65.1 (^{5}A′)
$Cr^+(CH_4)$	52.3 (^{4}A′)	58.3 (^{6}A′)
$Mn^+(CH_4)$	53.2 (^{5}A′)	65.5 (^{7}A′)
$Fe^+(CH_4)$	47.9 (^{4}A″)	59.2 (^{6}A′)
$Co^+(CH_4)$	46.0 (^{3}A″)	59.0 (^{5}A′)
$Ni^+(CH_4)$	48.4 (^{2}A′)	55.9 (^{4}A′)
$Cu^+(CH_4)$	47.9 (^{1}A′)	43.1 (^{3}A′)
ΔE_2		
$Sc^+(CH_4)$	41.3 (^{1}A′)	51.3 (^{3}A″)
$Ti^+(CH_4)$	46.7 (^{2}A″)	43.4 (^{4}A′)
$V^+(CH_4)$	49.2 (^{3}A′)	43.6 (^{5}A′)
$Cr^+(CH_4)$	29.3 (^{4}A′)	41.8 (^{6}A′)
$Mn^+(CH_4)$	41.5 (^{5}A′)	59.9 (^{7}A′)
$Fe^+(CH_4)$	23.4 (^{4}A″)	53.3 (^{6}A′)
$Co^+(CH_4)$	20.7 (^{3}A″)	51.2 (^{5}A′)
$Ni^+(CH_4)$	23.3 (^{2}A′)	45.0 (^{4}A′)
$Cu^+(CH_4)$	16.8 (^{1}A′)	35.0 (^{3}A′)

The symmetry labels indicated are for the transition states.

than 50 kcal mol^{-1} in the low-spin states of some methane complexes. These values, of course, include zero-point vibrational energy corrections. Note that the low-spin states of the late transition-metal ions and the high-spin state of the Cu^+ ion give values less than 50 kcal mol^{-1}. It is 43–48 kcal mol^{-1} on the $Fe^+(CH_4)$, $Co^+(CH_4)$, $Ni^+(CH_4)$, and $Cu^+(CH_4)$ complexes. These activation energies would still require high temperatures for the inversion of methane to be facile. Are such low-lying transition states thermally accessible or not? As each activation energy (ΔE_1) indicated in Table 1 involves the binding energy of the $M^+(CH_4)$ complex (16 kcal mol^{-1} on the average), the actual barrier height should be decreased by this quantity if measured from the dissociation limit. The internal energy of the reacting system is increased during the formation of the methane complex, and it can be used for the inversion of methane. Considering the adiabatic process, ΔE_2 is a substantial activation barrier to be considered. Therefore, the activation barrier for the inversion of methane is 17–23 kcal mol^{-1} on the late transition-metal complexes, $Fe^+(CH_4)$, $Co^+(CH_4)$, $Ni^+(CH_4)$, and $Cu^+(CH_4)$. From the computed ΔE_2 values it is predictable that the configuration of methane should be effectively inverted especially on the low-spin potential energy surfaces for Fe^+, Co^+, Ni^+, and Cu^+. Thus, the transition states should be thermally accessible.

We next look at optimized structures of the reactant (= product) and the transition state for the inversion of methane on the $M^+(CH_4)$ complexes. There are, in general, two kinds of preferred binding modes for methane, the η^2-H,H and η^3-H,H,H modes indicated in Chart 4. Although we do not show a dotted line between the carbon atom and the M^+ ion, this interaction from orbital interaction analyses is found to be important in the interaction between a hydrogen atom and the M^+ ion in the two binding modes. The η^1-H and η^2-C,H modes are rare. Most of the methane-complexes investigated take η^2-H,H and η^3-H,H,H modes, the low-spin states most likely prefer the η^2-H,H mode and the high-spin states the η^3-H,H,H mode.

Our B3LYP computations demonstrate that the $Fe^+(CH_4)$ complex exhibits η^2-H,H binding modes in both spin states, as shown in Fig. 4. The H–C–H angle near the Fe^+ ion was computed to be ca. 116° in both spin states of the $Fe^+(CH_4)$ complex. This structure is stabilized significantly by both the donor and the acceptor interactions. The Fe–C distance of the reactant (or product) complex is 2.373 Å in the quartet state and 2.780 Å in the sextet state, being in line with a general feature of transition-metal complexes, e.g. the metal–ligand distance in a high-spin state is longer than in a low-spin state. The computed transition states for the Fe^+ complex have a C_s structure, in which one pair of C–H bonds is 1.182 (1.187) Å in length and the other pair is 1.107 (1.109) Å in the quartet (sextet) state. The bond angle of H–C–H for the long C–H pair is 49.3° (48.6°), and for the short C–H pair is 97.9° (96.7°), in the quartet (sextet) state. The Fe–C distance decreases significantly in the transition state compared with that in the σ-complex, showing that the interaction between Fe^+ and CH_4 is significant in this electronic process. The imaginary frequency of 1610i cm^{-1} for free methane is shifted reasonably down to 968i cm^{-1} in the

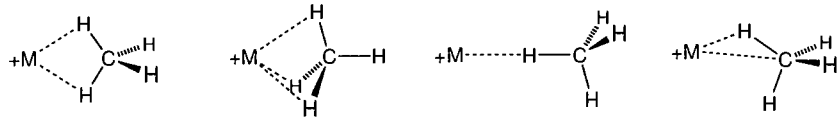

Chart 4.

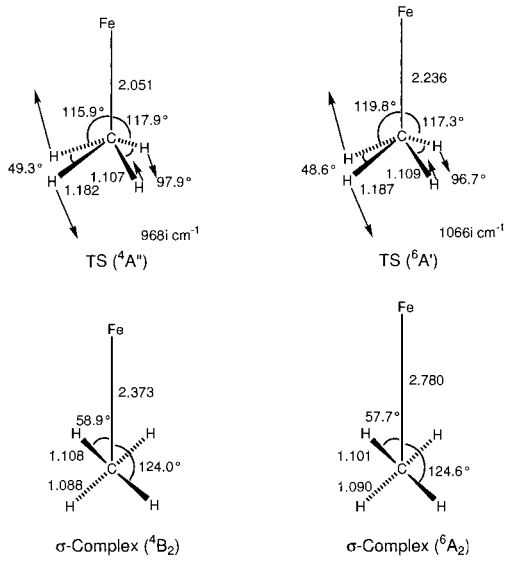

Fig. 4. Optimized structures of the σ complex (C_{2v}) and the transition state (C_s) for the inversion of methane on the $Fe^+(CH_4)$ complex. The bond lengths are in Å, and the bond angles (italic) are in degrees. The arrows in the transition states indicate the transition vector.

quartet state and 1066i cm^{-1} in the sextet state. This downshift of frequency corresponds to the lowering of the barrier height for the methane inversion. IRC analyses confirmed that the transition state correctly leads to the equivalent minimum in both the forward and reverse directions. Thus, the transition state shown in Fig. 4 is, in fact, the true transition state for the inversion of methane at the Fe^+ active center. If such an alkane-complex is formed as a reaction intermediate in C–H bond activation reactions, we expect that the inversion of the substrate at a carbon atom should occur reasonably, leading to stereochemical scrambling.

3.3. Orbital interaction analysis

To find a good reason why the barrier height for the inversion of methane is low on the low-spin states of the late transition-metal complexes $M^+(CH_4)$, we carried out a FMO analysis with the extended Hückel method. At the center of Fig. 5, the MOs of the C_s transition state are constructed from the MOs of the Fe^+ and the CH_4 fragments. The threefold degenerate t_2 HOMO of methane splits into one at -12 eV and two at -16 eV, according to the distortion of methane. The HOMO at -12 eV interacts with one of the 3d orbitals of the Fe^+ ion, leading to the in-phase combination at -14 eV (11a′) and the out-of-phase counterpart at -12 eV (14a′), while the two orbitals of methane at -16 eV do not interact with the Fe^+ ion. The in-phase one is doubly filled and the out-of-phase one singly filled. The 15a′ orbital, which comes mainly from the 4s and 4p orbitals of the Fe^+ ion, lies 4 eV above the d-block orbitals around -12 eV.

The sextet and the quartet states arise whether the 15a′ orbital at -8 eV is filled or not, respectively. From B3LYP calculations, the quartet transition state lies 10 kcal mol^{-1} below the sextet transition state in the $Fe^+(CH_4)$ complex. Although explicit electron–electron interactions are not included in the extended Hückel method, we can gain useful information about the preferred spin state from an empirical criterion

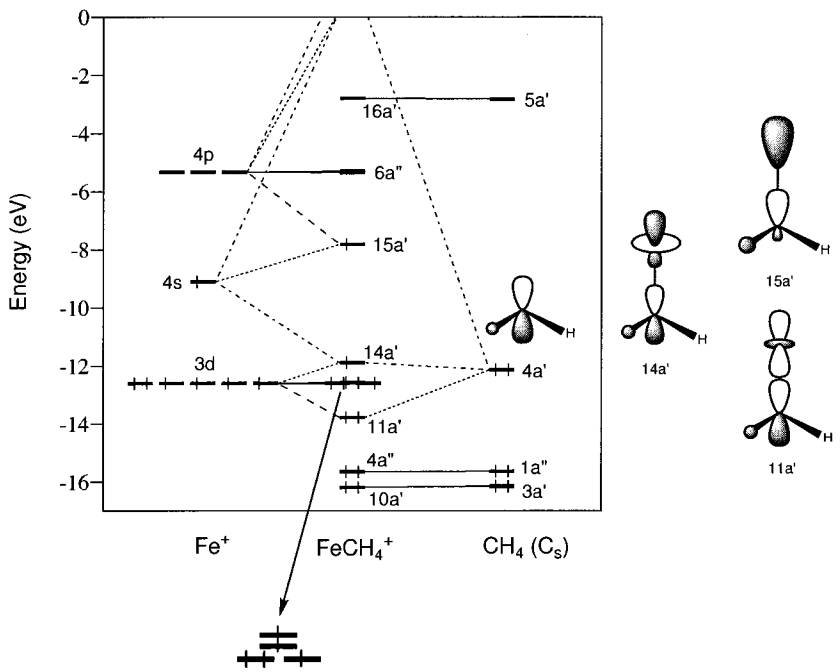

Fig. 5. A FMO analysis of the transition state for the inversion of methane on the $Fe^+(CH_4)$ complex. The spin state indicated is sextet.

within the framework of this one-electron theory. In general, a low-spin state is expected to occur in the extended Hückel method if energy splitting between the two levels is more than 1.5 eV [38]. Therefore, the low-spin quartet transition state is predicted to lie below the high-spin sextet transition state because the high-lying 15a′ orbital is vacant in the quartet state. By the same reasoning, the low-spin transition states of the $Co^+(CH_4)$, $Ni^+(CH_4)$, and $Cu^+(CH_4)$ complexes are more stable in energy than the corresponding high-spin transition states.

4. Conclusions

The inversion of methane has been an important subject in theoretical chemistry ever since the original work of Hoffmann, Alder, and Wilcox. We give another dimension to the potential meaning of this simple reaction. The DFT computations suggested that the inversion of methane could actually occur on the $M^+(CH_4)$ complexes, in which M^+ is the first-row transition-metal ions from Sc^+ to Cu^+. The transition states for the inversion of methane in these methane-complexes appear to have an interesting C_s structure in which one pair of C–H bonds is about 1.2 Å in length and the other pair is about 1.1 Å. The activation barrier for the inversion of methane was computed to be 17–23 kcal mol^{-1} on the late transition-metal complexes, $Fe^+(CH_4)$, $Co^+(CH_4)$, $Ni^+(CH_4)$, and $Cu^+(CH_4)$ at the B3LYP level of DFT. As these values are much smaller than those for the inversion of free methane (109 kcal mol^{-1}) and the energy required for C–H bond cleavage of methane (104 kcal mol^{-1}), the methane inversion can occur reasonably at the transition-metal active center of catalysts and enzymes through a sufficiently low-lying transition state if such a methane complex is formed during reactions. We consider that a radical mechanism may not be the sole source of the observed loss of stereochemistry in hydrocarbon hydroxylation reactions and the other related reactions catalyzed by transition-metal complexes and metalloenzymes.

Acknowledgements

The author thanks Yoshihito Shiota and Akiya Suzuki for computational assistance. This work was in part supported by a Grant-in-Aid for Scientific Research on the Priority Area 'Molecular Physical Chemistry' from the Ministry of Education, Science, Sports and Culture of Japan and the Iwatani Naoji Foundation's Research Grant. Computational time was provided by the Computer Center of the Institute for Molecular Science.

References

[1] (a) J.H. van't Hoff, Arch. Neerl. Sci. Exactes Nat. (1874) 445;
(b) J.A. LeBel, Bull. Soc. Chim. Fr. 22 (1874) 337;
(c) Review: D. Röttger, G. Erker, Angew. Chem. Int. Ed. Engl. 36 (1997) 812.
[2] R. Hoffmann, R.W. Alder, C.F. Wilcox Jr., J. Am. Chem. Soc. 92 (1970) 4992.
[3] T.A. Albright, J.K. Burdett, M.-H. Whangbo, Orbital Interactions in Chemistry, Wiley, New York, 1985.
[4] In an eight-electron AH_4 system, the HOMO is the a_{2u} or the b_{1g} orbital in a square-planar structure, and therefore they prefer to be tetrahedral rather than square planar.
[5] H.J. Monkhorst, Chem. Commun. (1968) 111.
[6] (a) J.B. Collins, J.D. Dill, E.D. Jemmis, Y. Apeloig, P.v.R. Schleyer, R. Seegger, J.A. Pople, J. Am. Chem. Soc. 98 (1976) 5419;
(b) M.-B. Krogh-Jespersen, J. Chandrasekhar, E.-U. Würthwein, J.B. Collins, P.v.R. Schleyer, J. Am. Chem. Soc. 102 (1980) 2263.
[7] M.S. Gordon, M.W. Schmidt, J. Am. Chem. Soc. 115 (1993) 7486.
[8] The matrix elements of Hessian (f_{ij}), termed quadratic force constant, are the second derivatives of the potential energy with respect to mass-weighted cartesian displacements, evaluated at the equilibrium nuclear configuration.
[9] M.J.M. Pepper, I. Shavitt, P.v.R. Schleyer, M.N. Glukhovtsev, R. Janoschek, M. Quack, J. Comput. Chem. 16 (1995) 207.
[10] (a) A. Author, in: P.R. Ortiz de Montellano (Ed.), Cytochrome P450: Structure, Mechanism, and Biochemistry, 2nd ed., Plenum Press, New York, 1995;
(b) M. Sono, M.P. Roach, E.D. Coulter, J.H. Dawson, Chem. Rev. 96 (1996) 2841.
[11] (a) B.J. Wallar, J.D. Lipscomb, Chem. Rev. 96 (1996) 2625;
(b) J.D. Lipscomb, Annu. Rev. Microbiol. 48 (1994) 371;
(c) A.L. Feig, S.J. Lippard, Chem. Rev. 94 (1994) 759;
(d) S.J. Lippard, Angew. Chem. Int. Ed. Engl. 27 (1988) 344;
(e) L. Que Jr., Y. Dong, Acc. Chem. Res. 29 (1996) 190.
[12] J.T. Groves, G.A. McClusky, R.E. White, M.J. Coon, Biochem. Biophys. Res. Commun. 81 (1978) 154.
[13] R.E. White, J.P. Miller, L.V. Favreau, A. Bhattacharyaa, J. Am. Chem. Soc. 108 (1986) 6024.
[14] (a) N.D. Priestley, H.D. Floss, W.A. Froland, J.D. Lipscomb, P.G. Williams, H. Morimoto, J. Am. Chem. Soc. 114 (1992) 7561;
(b) A.M. Valentine, B. Wilkinson, K.E. Liu, S. Komar-Panicucci, N.D. Priestley, P.G. Williams, H. Morimoto, H.G. Floss, S.J. Lippard, J. Am. Chem. Soc. 119 (1997) 1818.
[15] (a) P.E.M. Siegbahn, R.H. Crabtree, J. Am. Chem. Soc. 119 (1997) 3103;
(b) P.E.M. Siegbahn, Inorg. Chem. 38 (1999) 2880.
[16] (a) K. Yoshizawa, T. Ohta, Y. Shiota, T. Yamabe, Chem. Lett. (1997) 1213;
(b) K. Yoshizawa, T. Ohta, T. Yamabe, Bull. Chem. Soc. Jpn. 71 (1998) 1899;
(c) K. Yoshizawa, A. Suzuki, Y. Shiota, T. Yamabe, Bull. Chem. Soc. Jpn. 73 (2000) 815.
[17] H. Basch, K. Mogi, D.G. Musaev, K. Morokuma, J. Am. Chem. Soc. 121 (1999) 7249.
[18] B.D. Dunietz, M.D. Beachy, Y. Cao, D.A. Whittington, S.J. Lippard, R.A. Friesner, J. Am. Chem. Soc. 122 (2000) 2828.
[19] (a) D. Schröder, H. Schwarz, Angew. Chem. Int. Ed. Engl. 29 (1990) 1433;
(b) H. Schwarz, Angew. Chem. Int. Ed. Engl. 30 (1991) 820;
(c) D. Schröder, H. Schwarz, Angew. Chem. Int. Ed. Engl. 34 (1995) 1973.

[20] (a) K. Yoshizawa, Y. Shiota, T. Yamabe, Chem. Eur. J. 3 (1997) 1160;
(b) K. Yoshizawa, Y. Shiota, T. Yamabe, J. Am. Chem. Soc. 120 (1998) 564;
(c) K. Yoshizawa, Y. Shiota, T. Yamabe, Organometallics 17 (1998) 2825;
(d) Y. Shiota, K. Yoshizawa, J. Am. Chem. Soc. 122 (2000) 12317.
[21] (a) K. Yoshizawa, R. Hoffmann, Inorg. Chem. 35 (1996) 2409;
(b) K. Yoshizawa, T. Yamabe, R. Hoffmann, New J. Chem. 21 (1997) 151;
(c) K. Yoshizawa, T. Ohta, T. Yamabe, R. Hoffmann, J. Am. Chem. Soc. 119 (1997) 12311.
[22] L. Shu, J.C. Nesheim, K. Kauffmann, E. Münck, J.D. Lipscomb, L. Que Jr., Science 275 (1997) 515.
[23] (a) F. Ogliaro, N. Harris, S. Cohen, M. Filatov, S.P. de Visser, S. Shaik, J. Am. Chem. Soc. 122 (2000) 8977;
(b) N. Harris, S. Cohen, M. Filatov, F. Ogliaro, S. Shaik, Angew. Chem. Int. Ed. Engl. 39 (2000) 2003.
[24] (a) K. Yoshizawa, A. Suzuki, T. Yamabe, J. Am. Chem. Soc. 121 (1999) 5266;
(b) K. Yoshizawa, A. Suzuki, Chem. Phys. in press.
[25] (a) A.D. Becke, Phys. Rev. A 38 (1988) 3098;
(b) A.D. Becke, J. Chem. Phys. 98 (1993) 5648.
[26] C. Lee, W. Yang, R.G. Parr, Phys. Rev. B 37 (1988) 785.
[27] S.H. Vosko, L. Wilk, M. Nusair, Can. J. Phys. 58 (1980) 1200.
[28] J. Baker, M. Muir, J. Andzelm, A. Schemer, in: B.B. Laird, R.B. Ross, T. Ziegler (Eds.), Chemical Applications of Density-Functional Theory, ACS Symposium Series 629, American Chemical Society, Washington, DC, 1996.
[29] A.J.H. Wachters, J. Chem. Phys. 52 (1970) 1033.
[30] K. Raghavachari, G.W. Trucks, J. Chem. Phys. 91 (1989) 1062.
[31] R. Krishnan, J.S. Binkley, R. Seegar, J.A. Pople, J. Chem. Phys. 72 (1980) 650.
[32] M.J. Frisch, G.W. Trucks, H.B. Schlegel, P.M.W. Gill, B.G. Johnson, M.A. Robb, J.R. Cheeseman, T.A. Keith, G.A. Petersson, J.A. Montgomery, K. Raghavachari, M.A. Al-Laham, V.G. Zakrzewski, J.V. Ortiz, J.B. Foresman, J. Cioslowski, B.B. Stefanov, A. Nanayakkara, M. Challacombe, C.Y. Peng, P.Y. Ayala, W. Chen, M.W. Wong, J.L. Andres, E.S. Replogle, R. Gomperts, R.L. Martin, D.J. Fox, J.S. Binkley, D.J. Defrees, J. Baker, J.J.P. Stewart, M. Head-Gordon, C. Gonzalez, J.A. Pople, GAUSSIAN 94, Gaussian Inc., Pittsburgh, PA, 1995.
[33] (a) R. Hoffmann, J. Chem. Phys. 39 (1963) 1397;
(b) R. Hoffmann, W.N. Lipscomb, J. Chem. Phys. 36 (1962) 2179;
(c) R. Hoffmann, W.N. Lipscomb, J. Chem. Phys. 37 (1962) 2872.
[34] G.A. Landrum, YAeHMOP, Yet Another extended Hückel Molecular Orbital Package, version 2.0, Cornell University, Ithaca, New York, 1997.
[35] (a) K. Fukui, J. Phys. Chem. 74 (1970) 4161;
(b) K. Fukui, Acc. Chem. Res. 14 (1981) 363.
[36] (a) D.G. Musaev, N. Koga, K. Morokuma, J. Phys. Chem. 97 (1993) 4064;
(b) D.G. Musaev, K. Morokuma, N. Koga, K. Ngyen, M.S. Gordon, T.R. Cundari, J. Phys. Chem. 97 (1993) 11435;
(c) D.G. Musaev, K. Morokuma, J. Chem. Phys. 101 (1994) 10697;
(d) D.G. Musaev, K. Morokuma, J. Phys. Chem. 100 (1996) 11600.
[37] (a) D.J. Trevor, D.M. Cox, A. Kaldor, J. Am. Chem. Soc. 112 (1990) 3742;
(b) K.K. Irikura, J.L. Beauchamp, J. Phys. Chem. 95 (1991) 8344;
(c) Y.A. Ranasinghe, T.J. MacMahon, B.S. Freiser, J. Phys. Chem. 95 (1991) 7721;
(d) R.J. Van Zee, S. Li, W. Weltner Jr., J. Am. Chem. Soc. 115 (1993) 2976;
(e) J.J. Carrol, J.C. Weisshaar, J. Am. Chem. Soc. 115 (1993) 800;
(f) P. Burger, R.G. Bergman, J. Am. Chem. Soc. 115 (1993) 10462;
(g) C.P. Schaller, J.B. Bonanno, P.T. Wolczanski, J. Am. Chem. Soc. 116 (1994) 4133;
(h) X.-X. Zhang, B.B. Wayland, J. Am. Chem. Soc. 116 (1994) 7897;
(i) W.E. Billups, S.-C. Chang, R.H. Hauge, J.L. Margrave, J. Am. Chem. Soc. 117 (1995) 1387;
(j) P.A.M. van Koppen, P.R. Kemper, J.E. Bushnell, M.T. Bowers, J. Am. Chem. Soc. 117 (1995) 2098;
(k) M.L. Campbell, J. Am. Chem. Soc. 119 (1997) 5984.
[38] R. Hoffmann, G.D. Zeiss, G.W. Van Dine, J. Am. Chem. Soc. 90 (1968) 1485.